

Development and Validation of an Internet-Based Remote Perimeter (Perimouse)

Zidong Chen ^{1,*}, Xiaoyuan Shen ^{1,*}, Yuning Zhang ¹, Wenxin Yang¹, Jiexin Ye², Zhiqiang Ouyang², Guifeng Zheng², Yangfan Yang¹, and Minbin Yu ¹

¹ Sun Yat-Sen University, Zhongshan Ophthalmic Center, State Key Laboratory of Ophthalmology, Guangzhou, PR China

² Sun Yat-Sen University, School of Computer Science and Engineering, Guangzhou, PR China

Correspondence: Minbin Yu, State Key Laboratory of Ophthalmology, Zhongshan Ophthalmic Center, Sun Yat-Sen University, Guangzhou 510060, P.R. China. e-mail: yuminbin@mail.sysu.edu.cn

Received: September 11, 2023

Accepted: January 13, 2024

Published: March 20, 2024

Keywords: glaucoma; visual field test; internet-based intervention

Citation: Chen Z, Shen X, Zhang Y, Yang W, Ye J, Ouyang Z, Zheng G, Yang Y, Yu M. Development and validation of an internet-based remote perimeter (Perimouse). *Transl Vis Sci Technol.* 2024;13(3):16. <https://doi.org/10.1167/tvst.13.3.16>

Purpose: We sought to validate the feasibility of Perimouse, an internet-based remote perimeter that allows for natural fixation and can be performed on most computers via a web page.

Methods: In this cross-sectional study, Perimouse evaluated the visual field of 45 healthy people and 27 patients with primary open-angle glaucoma on a laptop. Participants used a mouse cursor to locate new dots on the screen that were determined by preset saccade vectors. A “click and confirm” strategy was used to eliminate the unwanted visual search. Dot brightness was either fixed at 12 dB in the suprathreshold program (screening program) or variable in the threshold program. We compared Perimouse outcomes with the Humphrey Field Analyzer (HFA) 24-2 Swedish Interactive Testing Algorithm standard program.

Results: In the screening program, Perimouse showed moderate to high concordance with HFA. The intraclass coefficient ranged from 0.58 to 0.86 in different areas of Garway-Heath mapping. In the threshold program, normal subjects had threshold ranging from 19 to 16 dB, presenting sensitivity changes according to the “hill of vision”. The test-retest difference was 0.09 dB. Habitual spectacle correction and environmental luminance (2–337 lux) had little impact on the central or peripheral threshold ($P > 0.05$). The correlation between Perimouse and HFA threshold sensitivity was strong ($R = 0.950$), although Perimouse mean defect was 4.40 dB higher than the HFA mean defect.

Conclusions: Perimouse is a reliable visual field test that correlates strongly with HFA. It shows potential for population screening and monitoring visual field defects.

Translational Relevance: Perimouse assesses the visual field using saccade vectors without eye trackers, enhancing its accessibility via a web page.

Introduction

Glaucoma, a leading cause of irreversible blindness, is estimated to affect 111.8 million adults between the ages of 40 and 80 years by 2040.¹ Despite its impact, more than 60% of cases in developed regions and more than 90% of cases in developing regions remain undetected.² This factor can be attributed to asymptomatic presentations in the early stages and limited access to high-quality and affordable eyecare.^{3–5} Vision loss caused by glaucoma is avoidable, and early screening and

treatment have demonstrated an increased diagnostic window of 5.1 to 8.6 years with significant cost effectiveness.^{6,7} However, implementing these measures remains challenging, particularly in remote and resource-limited areas. In addition, the coronavirus disease 2019 pandemic emphasizes the demand for remote alternatives in ophthalmic care. Home monitoring, combined with portable devices and artificial intelligence, has propelled this trend.⁸ Fortunately, the widespread availability of the Internet, especially in countries such as China, where coverage is at 70.4%, presents a unique opportunity for innovative health care solutions.⁹

Visual field testing, such as standard automated perimetry, is considered the clinical standard for diagnosing and monitoring the progression of glaucoma. It is a well-suited test to be performed via the Internet.¹⁰ Attempts have been made to implement visual field tests on web pages, such as the Spaeth/Richman Contrast Sensitivity test and the Peristat, and the Online Circular Contrast Perimetry test.^{11–14} Although good agreement between these novel perimetry tests and standard automated perimetry has been observed, concerns have been raised regarding the suprathreshold stimuli, which may limit their availability for mass screening.¹⁵ Moreover, they require the patient to sustain fixation on a visual target for several minutes, thus suppressing the foveation reflex that compels us to gaze directly at a fresh visual stimulus.¹⁶

Recently, several novel eye movement-based perimetry designs have been reported. These include saccadic vector optokinetic perimetry, Damato multifixation campimetry online, eyecatcher, and eye-tracking perimetry.^{17–19} Compared with traditional perimetry tests, these designs offer a more natural and intuitive testing experience that significantly improves testing comfort and enhances acceptance. Additionally, the use of free viewing in these designs further enhances their appeal and ease of use.

In the current study, we aimed to design a novel Internet-based perimetry (Perimouse) adopting this fixation alteration strategy, using both a suprathreshold program (screening program) and a threshold program. This study validates the feasibility of Perimouse and presents data acquired from normal controls and patients with glaucoma.

Materials and Methods

This observational, cross-sectional pilot investigation was conducted in the Zhongshan Ophthalmic Center. The ethics committees of the Zhongshan Ophthalmic Center (No. 2023KYPJ119) approved the study.

Participants

All study participants were recruited from the outpatient department and among medical students, and they had to meet specific inclusion and exclusion criteria. Inclusion criteria were age 18 years or older, best-corrected decimal visual acuity of 0.8 or greater, intraocular pressure of 21 mm Hg or less, and no history of ocular surgery, trauma, or inflammation in the past 3 years. Additional criteria for patients with primary open-angle glaucoma included

intraocular pressure peak of 22 mm Hg or greater without medication or normal intraocular pressure control with medication, typical glaucomatous optic nerve damage, retinal nerve fiber layer defects visible on optical coherence tomography, and visual field defects corresponding to optic nerve damage demonstrated by the Humphrey Field Analyzer (HFA) (24-2 Swedish Interactive Testing Algorithm [SITA] Standard procedure). All subjects signed an informed consent form and had a full understanding of the clinical trial before voluntarily participating.

Exclusion criteria included severe refractive media clouding, fundus disease, and previous eye surgery within 3 months.

Subjects were required to wear their habitual spectacle correction during the test, with white nontransparent patches used to occlude the untested eyes.

Apparatus

The testing was conducted in a dim room using a laptop (MacBook Air [13-inch, Early 2015], gamma value = 2.2), mouse, and Internet access. The computer's output luminance was calibrated to the highest level (300 cd/m²) using a test background color of RGB (100, 100, 100) and a luminance of 38 cd/m². The stimulus brightness range was from 38 to 300 cd/m², corresponding with an RGB range of 100 to 255. The website was <https://qgyzj.gzzoc.com/tpceshi/public/index/login>.

Perimouse Parameters

The stimuli were 0.52° and simulated HFA 24-2 strategy with 44 locations, including 2 blind spots. The mouse was replaced by a white circle with 1.56° and 100% contrast ratio. Each test included a preliminary physiological blind spot identification test and a main visual field test.

Each trial was initiated with a random stimulus, determined by a virtual saccade vector based on a 24-2 grid tailored to the participant's physiological blind spot. Participants were instructed to fixate on the stimulus and indicate their perception of any subsequent stimuli relative to it using the left or right mouse buttons. Special logic was used to illustrate the perception of any stimuli (Fig. 1). Initially, new dots appeared as white on the screen. Once detected and encircled by the mouse cursor, the color of the dot change to red. Participants identified the detection of a dot by left clicking on it, at which point the red dot turned yellow and another white dot appeared on the screen. If the participant noticed the new dot, they left clicked again on the yellow dot, turning it green, and continued to move the mouse to click on subsequent dots. This

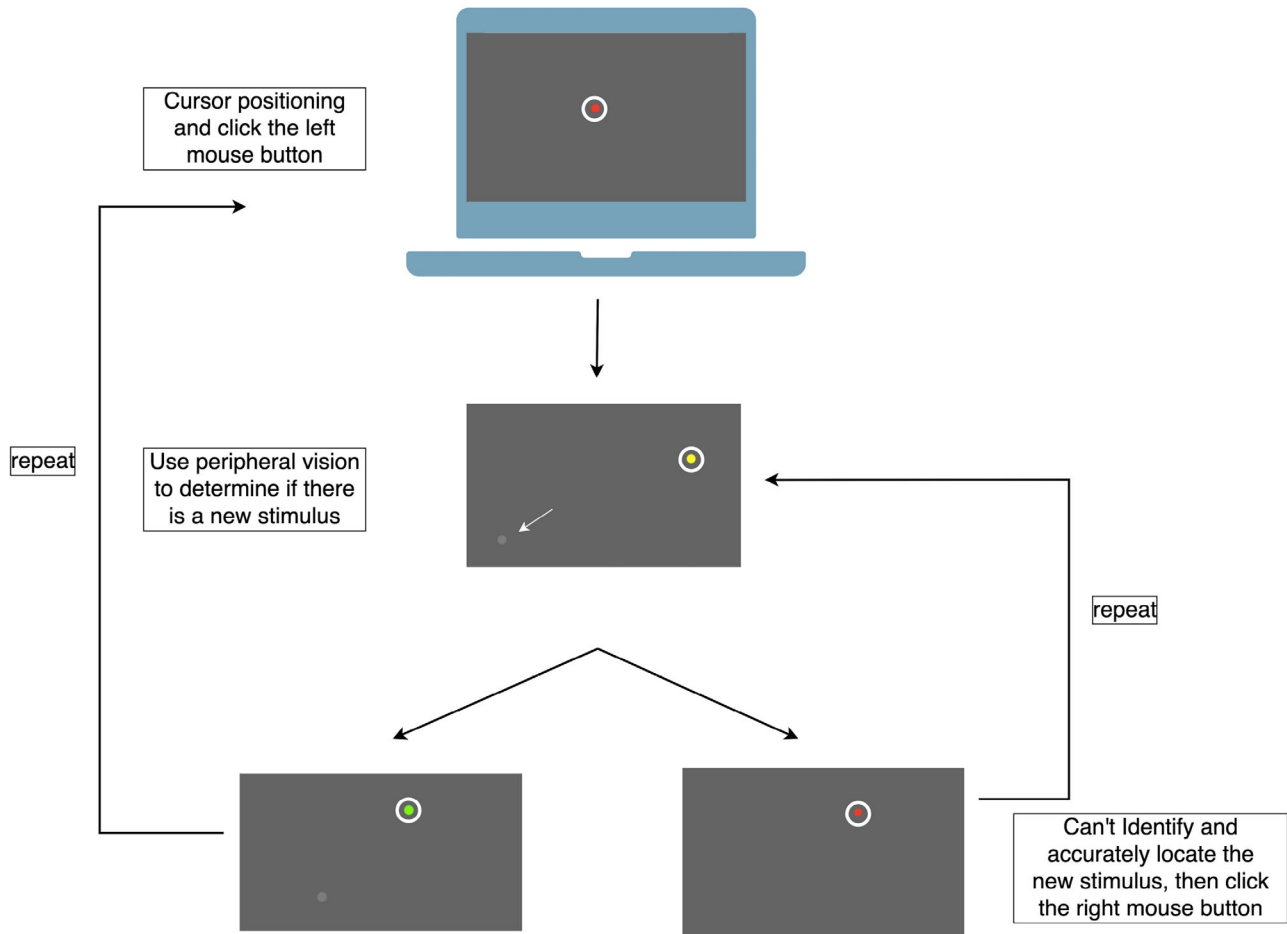


Figure 1. Diagram of the operation. The novel visual field test method requires desktop or laptop and mouse. During the test, a randomly selected point initially appears in gray-white. Upon positioning the cursor circle over this point, it transforms into red. By clicking the left mouse button, the red point transitions to yellow. At this point, another new dot has already appeared. Participants then use peripheral vision to judge its presence. If detected, participants click again with the left mouse button, turning the yellow dot green, then move the cursor to the new dot and repeat the test. If peripheral vision does not perceive a new dot, participants right click, turning the dot red, and simultaneously causing the newly appearing dot to disappear.

procedure was what we called a “click and confirm” strategy. If no new dot was observed, the participant right clicked to make a response. Additionally, for better understanding, we have attached a Supplementary Video titled “Operational Instructions.”

To optimize the program for clinical use, several modifications were made. First, when the current fixation failed to elicit perception for five consecutive newly presented stimuli, Perimouse automatically redirected gaze to the contralateral quadrant, thus expanding the visual field coverage in patients with severe loss. Additionally, to eliminate the involuntary visual search, the fixating dots disappeared if the mouse circle moved away. The test could be terminated by pressing the space bar, and untested points were distinguished as blue (screening program) or displayed with their current value (threshold program).

Determination of Physiological Blind Spots

The participant underwent a blind spot identification test before the main test. In the blind spot determination phase, a red cross remains stationary on the opposite side of the screen. A white dot with 100% contrast (RGB [255, 255, 255]) moved horizontally from the cross until it disappeared in the participant’s peripheral vision, mapping the blind spot. This step determined the ocular-to-screen distance, along with the magnitude of the vector connecting two random stimuli. It is essential to maintain this distance unchanged during the testing process to ensure accurate and reliable results. If the distance between the blind spot and the red cross surpasses a specified limit, a prompt will advise participants to “move forward” to keep the stimuli within the screen’s boundaries. Subsequently, to minimize head

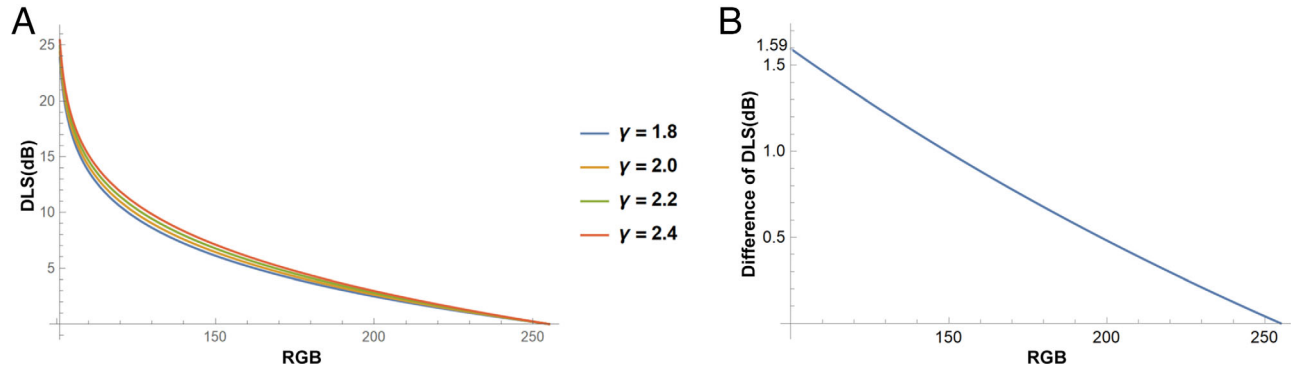


Figure 2. (A) The function curve between RGB, gamma value and DLS. (B) The function curve between RGB and DLS difference for $\gamma = 1.8$ and $\gamma = 2.4$. When RGB is (101, 101, 101), the maximum DLS difference is obtained, which is approximately 1.59 dB.

movements and maintain a consistent testing distance, participants were instructed to support their chin with one hand, while the elbow of the same arm rested on the tabletop.

Determination of Target Luminance and the Effect of Different Gamma

The test assumed gamma values from 1.8 to 2.4. The mapping between input luminance (gray scale) and output luminance was described by Equation (1) using the gamma lookup table: X represented the current gray level, γ denoted the gamma value, and L_{max} was the maximum output luminosity. The relationship between differential light sensitivity (DLS) and γ was expressed by Equation (2). The maximum DLS difference was 1.59 dB for RGB values (101, 101, 101) across different gamma values, as shown in Figure 2.

$$L_N = \left(\frac{X}{255} \right)^\gamma * L_{max} \quad (1)$$

$$DLS (dB) = 10 \lg \left(\frac{255^\gamma - 100^\gamma}{x^\gamma - 100^\gamma} \right) \quad (2)$$

Screening Program

Stimuli were presented once (except when the screen range limited the dots to be reset), with a 12-dB luminance. Responses were recorded as visible (white) or blind (black).

Threshold Program

The DLS was expressed using Equation (3), which was expressed with L_{max} , L_B , and L_S representing the luminance of the maximum, background, and stimulus, respectively, in the output.²⁰ The modified binary

search procedure was implemented to adjust light sensitivity while maintaining constant screen brightness.²¹ The threshold program commenced with a 12-dB stimulus and the logic flow is presented in Figure 3.

$$DLS (dB) = 10 * \lg \frac{L_{max} - L_B}{L_S - L_B} \quad (3)$$

Global Index

Fixation loss was defined as the number of instances when the mouse deviated after clicking on the yellow dot. False-positive rates were not documented because Perimouse's design did not replicate that of HFA. False-negative rates were assessed similarly to HFA, wherein six suprathreshold stimuli were tested. Reliability and visual field deficit were analysed using metrics such as fixation loss, false-negative rates, mean defect (MD), and mean sensitivity.

HFA Parameters

HFA with the 24-2 SITA was used to measure standard visual fields in both eyes. The glaucoma hemifield test results were classified as outside normal limits for all patients with glaucoma.^{19,22} HFA results were reliable (fixation loss of <20%, false-positive rates of <15%, and false-negative rates of <15%). Refractive error was determined by an auto refractor (KR-800, Topcon, Tokyo, Japan). The HFA MD values were used to measure glaucomatous disease severity.¹⁹

Testing Protocol

A normative database was established to determine the MD values for Perimouse using results obtained from healthy subjects. To assess reproducibility, one-

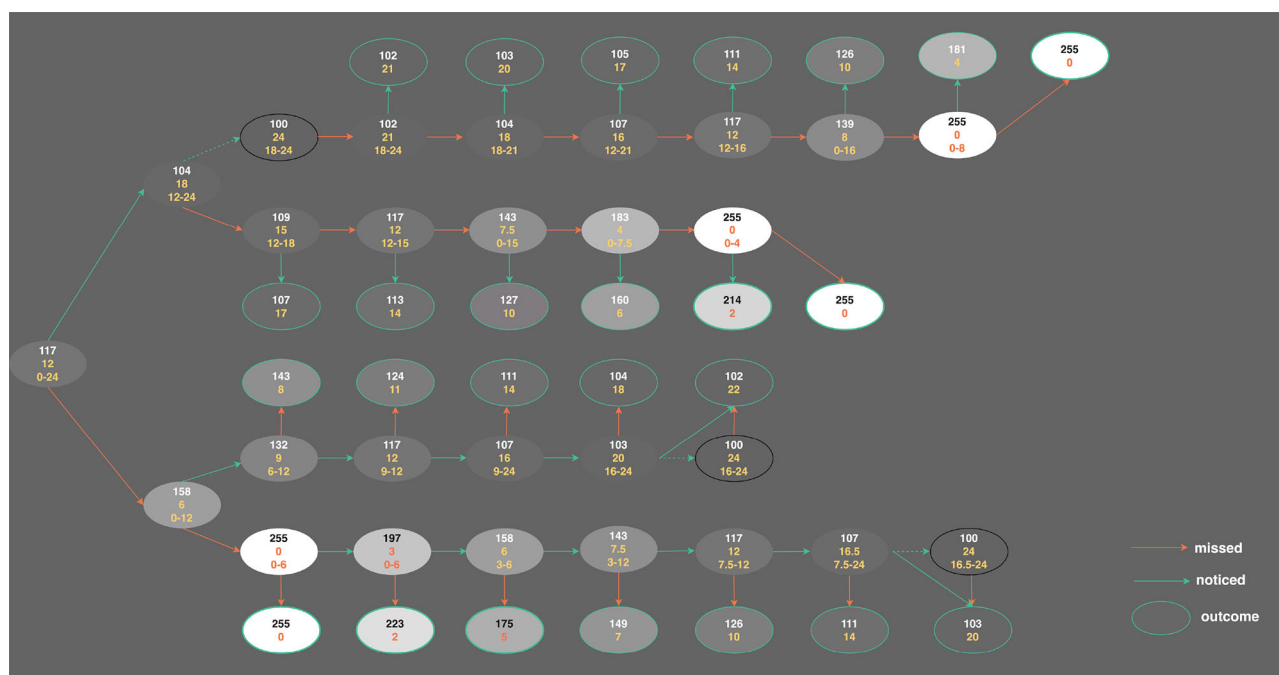


Figure 3. Threshold program protocol. The white or black three-digit numbers represent the RGB values of the stimuli. The yellow numbers correspond with the dB values, with the bottom number representing the range and the middle number indicating the current stimulus dB value. Following a simulation of the modified binary search procedure strategy, the following steps were implemented. Stimulation was conducted as 12 dB and the subsequent range selection was determined based on the subject's perceptual response. If the subject perceived (noticed) the stimulus, the dB range selected for the next stimulation interval was greater than the median value. Conversely, if the subject did not respond (missed), the dB range selected was smaller than the median value. If two consecutive stimuli at the same location resulted in perceptual response from the subject, the maximum value within the range was chosen to estimate the threshold. In contrast, if two consecutive stimuli failed to elicit a response, the minimum boundary of the range was used for threshold estimation.

half of the subjects were selected randomly for repeat testing. The impact of refractive error blur and ambient background light intensity on the test results was investigated. Furthermore, a key aspect of our methodology was the evaluation of test consistency across two quite different computers.

To compare the consistency of the Perimouse and HFA tests, we performed both tests on patients with glaucoma, either on the more advanced eye or both eyes, in a randomized order with a minimum interval of 10 minutes between the two tests.

Statistical Methods

We used the Shapiro–Wilk normality test to decide whether to perform parametric or nonparametric tests. For nonparametric data, continuous variables were presented as median with interquartile range, and for parametric data, mean \pm standard deviation was used. IBM SPSS Statistics version 22 (IBM Corp, Armonk, New York, USA) was used for statistical analyses. All tests were considered two tailed, and statistical significance was defined as a *P* value of less than 0.05. Functions were performed using Mathematica

(12.3 2021). The repeatability of Perimouse results was analyzed using the Wilcoxon signed ranks test and the Bland–Altman plot. The Student *t* test was performed to compare the effect factors. To more precisely locate the areas of visual field defects, we used the Garway Heath map to calculate the intraclass coefficient (ICC) values between the number of missed points in the Perimouse screening program, test and the number of points in the HFA total deviation probability plot that were less than 0.5% in different regions.²³ Spearman's rank correlation coefficient was used to assess the correlation of Perimouse with HFA.

Results

We assessed 47 normal subjects and 29 primary patients with glaucoma. Two normal subjects were excluded owing to an enlarged physiological blind spot, and two patients were excluded for failing to meet reliable HFA criteria. In total, 85 eyes from 45 normal subjects (95.7%) and 29 eyes from 27 patients (93.1%) were enrolled in the study. The clinical characteris-

Table. Participant Demographics

Clinical Characteristics

Controls	
Test subjects	45
Eyes (left/right)	85 (43/42)
Age, years, mean \pm standard deviation	27.53 ± 1.44
Sex (male/female)	22/23
Patients	
Test subjects	27
Eyes (left/right)	29 (10/19)
Age, years, mean \pm standard deviation	38.96 ± 2.42
Sex (male/female)	16/11
Severity (n, %)	
Mild	7 (24.1)
Moderate	10 (34.5)
Severe	12 (41.4)

Patients with glaucoma ($n = 27$) subdivided into mild (HFA MD > -6 dB, $n = 7$), moderate (-12 dB $<$ HFA MD < -6 dB, $n = 10$), or severe (HFA MD < -12 dB, $n = 12$).

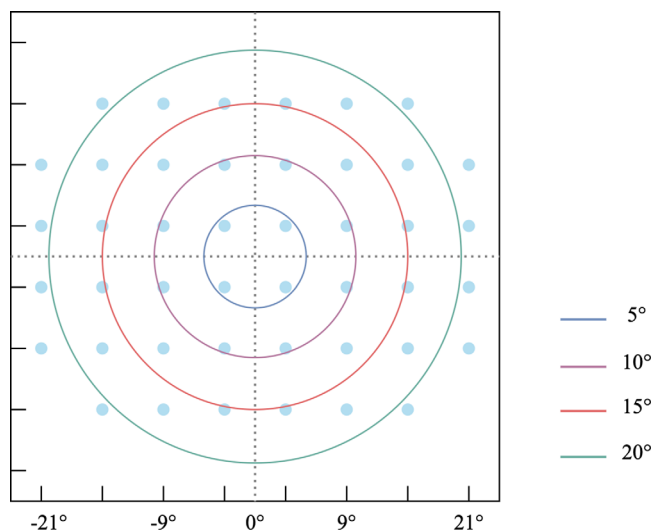


Figure 4. Test grid. Perimouse simulated the HFA 24-2 pattern, with the physiological blind spot positioned at 15° temporal and $\pm 3^\circ$ vertically from the fixation point.

tics of the study participants are presented in Table. Healthy subjects were found to be younger than those with glaucoma (27.53 ± 1.44 vs 38.96 ± 2.42 , respectively; $P < 0.001$).

Normative Database and Test-Retest Reliability

Distribution of loci in Perimouse were shown in Figure 4. Figures 5A and B present the screening program and threshold program results, respectively, for normal individuals. A total of 45 normal

subjects were tested to establish the DLS values for each locus, which served as a baseline to determine MD values, as depicted in Figure 5C. The left eye results were mirrored onto the corresponding locations of the right eye. In normal controls, the MD value was 0.00 ± 0.16 dB. The DLS of Perimouse decreased linearly as the eccentricity increased, as illustrated in Figure 5D. In terms of point-wise DLS between the test and retest, the Wilcoxon signed ranks test showed no significant differences ($P = 0.172$). Additionally, the Bland-Altman plot in Figure 5E illustrated the difference between test and retest performance for all controls and patients. The 95% limits of agreement were relatively narrow, indicating minimal variability in individual DLS, except for four extreme outliers among the severe patients. Point-wise DLS was compared between two different devices, a MacBook Air (Mac) and a Hewlett-Packard (HP, Pavilion 14-inch) computer. Notably, the HP computer exhibited a higher gamma value and maximum screen brightness. During the tests, the screen brightness of the HP was measured at approximately 100 lux using a handheld illuminometer (Aicevoos Digital Light Meter), whereas the Mac's screen brightness was approximately 30 lux. The Wilcoxon signed ranks test revealed significant differences in point-wise DLS between these two devices ($P < 0.05$). Furthermore, Figure 5F displayed a Bland-Altman plot that revealed a mean difference of -1.30 dB between the devices.

Effect of Habitual Spectacle Correction and Environmental Luminance

Figure 6 summarizes the effect of visual blur and environmental luminance on average light sensitivity thresholds for central (0° – 5°) and peripheral ($>5^\circ$) locations in normal controls. Neither visual blur nor room light had a significant effect on thresholds at both central and peripheral locations ($P > 0.05$).

Comparison of Perimouse and HFA in Patients With Glaucoma

The results of the screening and threshold programs in a typical patient with glaucoma were shown in Figure 7A to D. In terms of pointwise DLS values, the Bland-Altman plot (Fig. 8A) indicated that the results were stable, with Perimouse being approximately 15 dB less than HFA and having relatively tight limits of agreement. ICC between the two tests was up to 0.93.

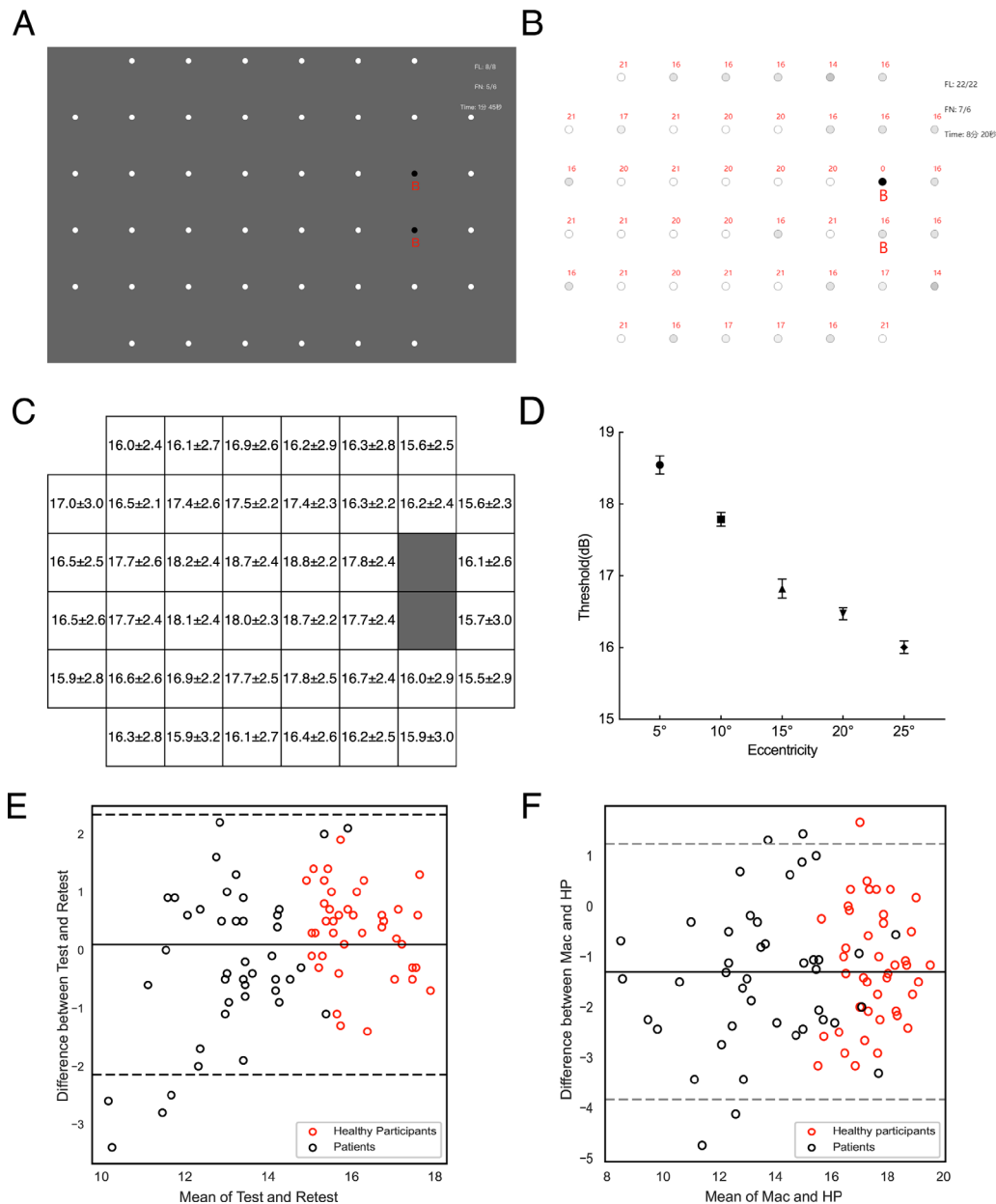


Figure 5. (A) and (B) The Perimouse outcomes of screening program and threshold program in normal person, respectively. “B” means the site of physiological blind spots. (C) The Perimouse threshold program. (D) The gradual decrease of the threshold with the increase of eccentricity. (E) and (F) Bland–Altman plots to evaluate Perimouse consistency and equipment agreement. In both plots, healthy participants were denoted by red hollow circles, while patients were represented by black hollow circles. (E) Test and retest repeatability in normal participants and patients with primary open-angle glaucoma. In the Bland–Altman plot, the upper and lower two dash lines indicated 95% limits of agreement (LOA) 2.33B and -2.14 dB, solid line showed a minimal bias of 0.09 dB. Four points (4.76%) occurred outside of the limits of agreement. (F) Agreement between measurements from Mac and HP. The solid line indicated the mean difference of -1.30 dB between the two quite different devices, and the upper and lower dashed lines represent the 95% limits of agreement at 1.23 dB and -3.84 dB, respectively. Five points (5.95%) occurred outside of the limits of agreement.

In the threshold program, a significant positive correlation (Spearman’s rank correlation coefficient $R = 0.950$; $P < 0.001$) was observed between Perimouse MD and HFA MD in patients with glaucoma. The relationship between Perimouse MD and HFA MD

was modelled using linear regression analysis to provide the following equation: $MD_{HFA} = MD_{Perimouse} \times 1.978 - 1.612$, as depicted in Figure 8B. The Bland–Altman analysis of global indices (MD) demonstrated acceptable variability between Perimouse and

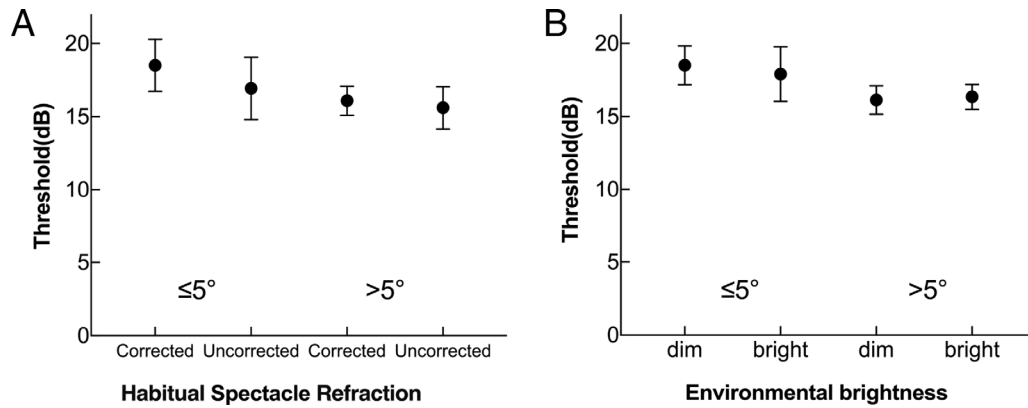


Figure 6. Effect of varying test conditions on light sensitivity thresholds at central (0° – 5°) and peripheral ($>5^\circ$) sites in normal subjects, respectively. **(A)** The presence or absence of the habitual wearing of glasses didn't have a significant effect on the light sensitivity threshold at the central ($P = 0.07$) or peripheral ($P = 0.273$) sites within a range of ± 3 D of refractive error. **(B)** Variation in ambient room lighting (from 2 to 337 lux) had little impact on the central ($P = 0.218$) or peripheral ($P = 0.477$) threshold.

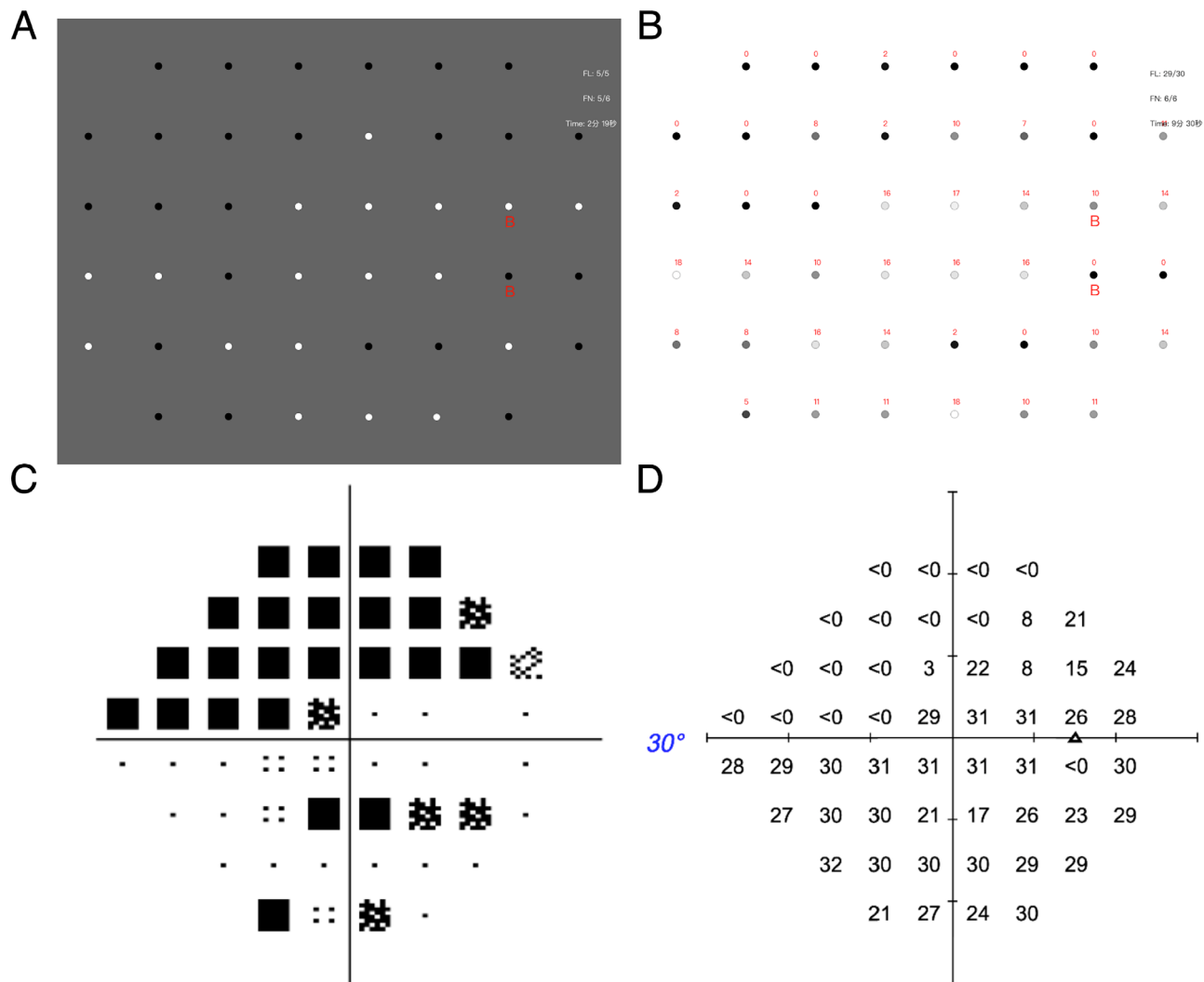


Figure 7. Visual field test results of a primary open-angle glaucoma patient using Perimouse and HFA SITA 24-2. **(A)** Perimouse screening procedure. **(B)** Perimouse threshold procedure. The red numbers represented DLs. **(C)** HFA 24-2 total deviation probability plot. **(D)** HFA 24-2 threshold test plot.



translational vision science & technology-

HFA in both glaucoma and control groups, as shown in Figure 8C. On average, the MD obtained by Perimouse was found to be 4.40 dB higher than that obtained by HFA. The difference between the two tests was variable and decreased with increasing average MD values, indicating higher agreement with milder visual field defect.

The ICC for the screening program of Perimouse and the total deviation probability plot of HFA in different areas of Garway–Heath mapping were shown in Figure 8D, indicating a moderate to strong correlation between the two tests with ICC values ranging from 0.58 to 0.86. Lower agreement was observed between the two tests in the loci around the physiological blind spot. Mean and standard deviation of pointwise threshold in patients were presented in Figures 8E and F, comparing the Perimouse with HFA, respectively.

Test Duration

In this study, the mean test duration for normal participants was 4.32 ± 0.28 minutes for the SITA Standard 24-2, 1.82 ± 0.07 minutes for the Perimouse screening program, and 7.07 ± 0.3 minutes for the Perimouse threshold program. Statistical analysis revealed that the Perimouse screening program demonstrated a significantly shorter test duration than HFA by 2.5 ± 1.82 minutes ($P < 0.05$), whereas the Perimouse threshold program was longer than HFA by 2.71 ± 2.33 minutes ($P < 0.05$).

For patients with glaucoma, the SITA Standard 24-2 showed a mean test duration of 6.15 ± 0.27 minutes. The Perimouse screening and threshold programs had mean durations of 5.42 ± 0.45 minutes and 11.55 ± 0.57 minutes, respectively. No significant differences were found between patients' Perimouse screening program and HFA, but there were significant differences in threshold program and HFA, with the former being 5.4 ± 3.42 minutes longer.

Discussion

In this article, we presented the development of a novel web-based perimetry test with unique features and evaluate its reliability by comparing it with Humphrey perimetry in normal subjects and participants with glaucoma. Our study explored the potential effect of screen parameters on DLS. Results show moderate agreement between Perimouse and HFA tests in both screening and threshold programs, demonstrat-

ing its potential as an useful tool for detecting visual field abnormalities.

Our results, depicted in Figure 2, demonstrated that the Perimouse maintained its precision across a range of gamma settings ($\gamma = 1.8$ to $\gamma = 2.4$). Variations in screen maximum output luminance had a negligible impact on the DLS measurements, confirming the tool's reliability. Specifically, we observed a significant DLS difference of 1.59 dB with the minimum RGB settings (101, 101, 101), according to the threshold protocol (Fig. 3). Our findings suggested that, in real-world scenarios, variations in maximum screen brightness and gamma values may impact DLS measurements. Specifically, screens with lower maximum brightness and gamma values are inclined to underestimate DLS, which could result in an overestimation of MD loss, highlighting the importance of considering these factors in threshold assessments.

We refined our testing parameters and established expected results for normal eyes following the typical hill of vision. Bland–Altman analysis showed strong agreement with a bias of approximately 0.09 dB (Fig. 5E), demonstrating the reproducibility and stability of Perimouse measurements. The robustness of Perimouse outcomes was minimally impacted by factors such as refractive error blur and ambient illumination, as depicted in Figure 6.

Our findings demonstrate the feasibility and reliability of using Perimouse for measuring visual field defects in both patients with glaucoma and population screening. Although the threshold values obtained using Perimouse were approximately 15 dB lower than those obtained with the HFA, the two tests showed good alignment. This discrepancy can be attributed to inherent differences between the devices, similar to the results obtained with another device, the Eyecatcher.¹⁸ The maximum brightness of stimuli generated by the HFA is 3183.1 cd/m², whereas the current computer has a limit of 300 cd/m², resulting in different maximum sensitivities between the devices. As a consequence of these different sensitivities, with the visual field defect increased, the MD values of both tests became progressively larger, particularly overestimating in severe cases. This trend highlights the need for integrating probability maps into Perimouse for more precise assessments. Perimouse demonstrated a correlational relationship with HFA in both screening and threshold programs (Fig. 8). Healthy individuals completed the screening or threshold program tests more quickly than patients, likely owing to their youth and superior computer proficiency. Although the Perimouse threshold program took longer than the HFA, it was accompanied by a relatively lower

incidence of fatigue complaints owing to the flexibility offered by altering fixation, as noted in personal communications.

The Perimouse provides several notable advantages. First, our findings are consistent with prior research on perimetry methods that involve altering fixation, such as Eyecatcher and saccadic vector optokinetic perimetry. These techniques have been demonstrated to exhibit good consistency in comparison to traditional perimetry.^{24–26} The fixation-altering feature enables a comprehensive evaluation of the visual field without hindering the foveation reflex. Second, unlike Damato multifixation campimetry online, which uses fixed high-contrast black-on-white stimuli,²⁴ or Peristat, which incorporates four different standardized levels of intensity,²⁶ Perimouse encompasses both screening and threshold programs. Therefore, it has the potential for use not only in mass screenings, but also in home monitoring. Third, the Perimouse measures light sensitivity in an HFA 24-2 grid, allowing for point-to-point comparison with the results of HFA. Furthermore, there is no limit to the reaction time to stimuli presented in the Perimouse, making it easier for elderly patients to use.²⁷

This study has several limitations that must be acknowledged. First, the sample size was relatively small, which restricts the ability to make definitive conclusions regarding the disease's severity. Further research using larger cohorts is required to assess the Perimouse's validity and its applicability to a broader population. Second, although the study assessed Perimouse in a clinical setting, additional evaluation is necessary to determine its feasibility in a home-based environment. Finally, as a tangential screen, there may be a disparity between the virtual and real location. However, the maximum estimated difference between the two is only 6%, which can be regarded as insignificant.

In conclusion, this study offers a comprehensive overview of the development of Perimouse and demonstrates its agreement with Humphrey visual field in both normal and glaucoma participants. This Internet-based approach could potentially provide an effective tool for patients with glaucoma in both screening and self-management.

Acknowledgments

The authors thank Zhonglun Cao (Department of Mathematical Sciences, Tsinghua University) for his valuable contribution in the data analysis by Mathematica.

Funded by Innovative Clinical Technique of Guangzhou (2024P-GX07).

Data Availability Statements: Data are available upon reasonable request. The complete source is available online at <https://qgyzj.gzzoc.com/tpceshi/public/index/login>, and is free for noncommercial use. All data relevant to the study are included in the article. All data analyzed during the study are included in this manuscript. Further enquiries can be directed to the corresponding author.

Disclosure: Z. Chen, None; X. Shen, None; Y. Zhang, None; W. Yang, None; J. Ye, None; Z. Ouyang, None; G. Zheng, None; Y. Yang, None; M. Yu, None

* ZC and XS contributed equally to this article.

References

1. Tham Y-C, Li X, Wong TY, et al. Global prevalence of glaucoma and projections of glaucoma burden through 2040: a systematic review and meta-analysis. *Ophthalmology*. 2014;121(11):2081–2090.
2. Soh Z, Yu M, Betzler BK, et al. The global extent of undetected glaucoma in adults: a systematic review and meta-analysis. *Ophthalmology*. 2021;128(10):1393–1404.
3. Kyari F, Entekume G, Rabiou M, et al. A Population-based survey of the prevalence and types of glaucoma in Nigeria: results from the Nigeria National Blindness and Visual Impairment Survey. *BMC Ophthalmol*. 2015;15:176.
4. Vijaya L, George R, Baskaran M, et al. Prevalence of primary open-angle glaucoma in an urban south Indian population and comparison with a rural population. The Chennai Glaucoma Study. *Ophthalmology*. 2008;115:648–654.
5. Prevalence, risk factors, and visual features of undiagnosed glaucoma: the Singapore Epidemiology of Eye Diseases study. *JAMA Ophthalmol*. 2015;133(8):938–946. Published online 2015:9.
6. Liang Y, Jiang J, Ou W, et al. Effect of community screening on the demographic makeup and clinical severity of glaucoma patients receiving care in urban China. *Am J Ophthalmol*. 2018;195:1–7.
7. Flaxman SR, Bourne RRA, Resnikoff S, et al. Global causes of blindness and distance vision impairment 1990–2020: a systematic review and meta-analysis. *Lancet Glob Health*. 2017;5(12):e1221–e1234.

8. Lee GA, Kong GYX, Liu C. Visual fields in glaucoma: where are we now? *Clinical Exp Ophthalmol*. 2023;51(2):162–169.
9. Industry PHE. *China Internet Development Report 2020: Blue Book for World Internet Conference*. Springer Nature Singapore; 2022, https://books.google.com/books?id=iat_EAAAQBAJ.
10. Wall M. What's new in perimetry. *J Neuroophthalmol*. 2004;24(1):46–55.
11. Sun Y, Erdem E, Lyu A, et al. The SPARCS: a novel assessment of contrast sensitivity and its reliability in patients with corrected refractive error. *Br J Ophthalmol*. 2016;100(10):1421–1426.
12. Daka Q, Mustafa R, Nezirli B, Virgili G, Azuara-Blanco A. Home-based perimetry for glaucoma: where are we now? *J Glaucoma*. 2022;31(6):361–374.
13. Ianchulev T, Pham P, Makarov V, Francis B, Minckler D. Peristat: a computer-based perimetry self-test for cost-effective population screening of glaucoma. *Curr Eye Res*. 2005;30(1):1–6.
14. Skalicky SE, Bigirimana D, Busija L. Online circular contrast perimetry via a web-application: optimising parameters and establishing a normative database. *Eye*. 2023;37:1184–1190.
15. Ichhpujani P, Thakur S, Sahi R, Kumar S. Validating tablet perimetry against standard Humphrey Visual Field Analyzer for glaucoma screening in Indian population. *Indian J Ophthalmol*. 2021; 69(1):87.
16. Damato B. Multifixation campimetry on line: a perimeter for the detection of visual field loss using the internet. *Br J Ophthalmol*. 2003;87(10):1296–1298.
17. Murray I, Perperidis A, Brash H, et al. Saccadic vector optokinetic perimetry (SVOP): a novel technique for automated static perimetry in children using eye tracking. *Annu Int Conf IEEE Eng Med Biol Soc*. 2013;2013:3186–3189.
18. Jones PR. An open-source static threshold perimetry test using remote eye-tracking (Eyecatcher): description, validation, and preliminary normative data. *Transl Vis Sci Technol*. 2020;9(8):18.
19. Jones PR, Smith ND, Bi W, Crabb DP. Portable perimetry using eye-tracking on a tablet computer—a feasibility assessment. *Transl Vis Sci Technol*. 2019;8(1):17.
20. Haigh A, Aphthorp D, Bizo LA. The role of Weber's law in human time perception. *Atten Percept Psychophys*. 2021;83(1):435–447.
21. Turpin A, McKendrick AM, Johnson CA, Vingrys AJ. Development of efficient threshold strategies for frequency doubling technology perimetry using computer simulation. *Invest Ophthalmol Vis Sci*. 2002;43(2):322–331.
22. Asman P, Heijl A. Glaucoma hemifield test. Automated visual field evaluation. *Arch Ophthalmol*. 1992;110(6):812–819.
23. Garway-Heath DF, Poinoosawmy D, Fitzke FW, Hitchings RA. Mapping the visual field to the optic disc in normal tension glaucoma eyes. *Ophthalmology*. 2000;107(10):1809–1815.
24. Olsen AS, Alberti M, Serup L, la Cour M, Damato B, Kolko M. Glaucoma detection with Damato multifixation campimetry online. *Eye*. 2016;30(5):731–739.
25. Olsen AS, Steensberg AT, la Cour M, et al. Can DMCO detect visual field loss in neurological patients? A secondary validation study. *Ophthalmic Res*. 2017;58(2):85–93.
26. Lowry EA, Hou J, Hennein L, et al. Comparison of Peristat online perimetry with the Humphrey perimetry in a clinic-based setting. *Transl Vis Sci Technol*. 2016;5(4):4.
27. Woods DL, Wyma JM, Yund EW, et al. Age-related slowing of response selection and production in a visual choice reaction time task. *Front Hum Neurosci*. 2015;9:193.